2013 American Control Conference (ACC)
Washington, DC, USA, June 17-19, 2013

Distributed Network Localization Using Angle-of-Arrival Information Part II: Discrete-Time Algorithm and Error Analysis

Guangwei Zhu, Jianghai Hu

Abstract— **In this paper, we propose a discrete-time distributed algorithm for network localization based on angle-of-arrival (AOA) measurements. This algorithm can be viewed as a special case of the averaging consensus algorithm in the two-dimensional space. We also analyze the localization error under inaccurate anchor positions and angles measurements and provide approximate formulae for the error terms. The effectiveness of our localization algorithm and error assessment tools is demonstrated through numerical examples. The main contribution of our paper lies in the theoretical framework for analyzing AOA-based localization processes as well as assessing localization error.**

Index Terms— **localization, angle-of-arrival (AOA), estimation, stiffness matrix, optimization, distributed algorithm**

I. Introduction

Localization of agents is one of the primary functionalities for numerous multi-agent systems, such as camera networks [2], environmental surveillance networks [3] and many other sensor/robot networks. These systems often require only low resolution localization results, and consist of a large number of wireless nodes. In order to reduce cost and energy consumption, localization is often done through relative measurements among the nodes instead of absolute positioning systems such as GPS, with the exception of a few nodes. These special nodes, which are often referred to as *anchors* or *beacons*, can provide absolute position reference for other nodes in the network.

Localization has long been an active research topic in the multi-agent systems field [4]. A majority of the existing works on the subject study the mechanisms of recovering node positions from relative distance measurements [5], [6], [7]. As was argued in Part I of this topic [1], it is also possible for a node to locate itself in the network by measuring the *directions* (a.k.a. angle-of-arrival, or AOA) of its neighboring nodes. Assuming that the angle measurements are aligned with a global orientation (e.g. define north to be 0°) for the network, Ash et al. [8] and Eren et al.[9] showed that given a minimal set of anchor nodes, the network can be very easily localized by computing the null space of the rigidity matrix in the two-dimensional scenario. The drawback of the direction-based methods, however, is that measuring angles may require more costly hardware. Nevertheless, in many environmental surveillance networks, the built-in cameras or acoustic sensors already provide the functionality of angle measurement [10]. As a result, direction-based localization via such devices becomes a natural extension.

In this paper, the AOA localization problem is formulated and solved through a matrix-theoretic approach. Although a similar approach was previously proposed and employed in [8], [9] to study the AOA localization problem, in this paper we provide an alternative solution to the AOA localization problem using the concept of *stiffness matrix* [11]. There are at least two advantages of this approach. One advantage is that a distributed consensus-like algorithm can be easily derived from the stiffness matrix using a matrix splitting technique. We show that the algorithm is very easy to implement in a distributed manner and proven to converge. A second advantage is that, since the stiffness matrix is square, some closed-form expressions can be derived using matrix calculus to quantify the localization errors caused by inaccurate anchor node positions and/or angle measurements. In addition to error analysis, these expressions could be useful for designing optimal formations, which can be obtained by minimizing these errors.

The organization of this paper is as follows. Some preliminaries of formation graph theory are introduced in Section II. Then in Section III, we formulate the AOA localization problem and deduce its analytic solution. We also show that the AOA localizability is equivalent to the infinitesimal rigidity [12], [13]. In Section IV we propose a distributed discrete-time algorithm to iteratively compute the solution of the AOA localization problem and prove its convergence. Simulation results are also provided to demonstrate its effectiveness. In Section V, the localization error resulted from inaccurate anchor positions or angle measurements is analyzed, and numerical examples are given. We conclude this paper and provide some future directions for improving the performance of the algorithm VI.

A. Notation

For symmetric matrices A, B, we write $A \succeq 0$ if A is positive semidefinite. For $\mathbf{v} = [a\ b]^\top \in \mathbb{R}^2$, we use the notation $\angle\mathbf{v}$ to denote the principal value of argument (within the range $[0, 2\pi)$) of the complex number $a + bi$ in the complex plane. We denote by $\mathbf{v}^\perp$ the vector $\mathbf{v}$ rotated by 90 degrees counterclockwise on the $\mathbb{R}^2$ plane. If $\mathbf{v}$ is a stacked vector consists of multiple two-dimensional subvectors, then $\mathbf{v}^\perp$ denotes the rotation applied on every individual two-dimensional subvector of $\mathbf{v}$. We also define the linear rotation operator $Q : \mathbf{p} \mapsto \mathbf{p}^\perp$ and $\mathbf{p}^\perp \mapsto -\mathbf{p}$, where the dimensions of the underlying spaces depend on the context.

Guangwei Zhu and Jianghai Hu are with the School of Electrical and Computer Engineering, Purdue University, West Lafayette, IN 47907, USA {guangwei,jianghai}@purdue.edu This work was partially supported by the NSF under Grant CNS-0643805.

Part I of the topic can be found in [1].

II. Formation Graph

In this section, we briefly introduce the notations of *formation graphs*, which are a natural tool to study multi-agent systems formation, including localization problems. Throughout the paper we assume the underlying space to be $\mathbb{R}^2$.

Definition 1 (Formation Graph): A formation graph, denoted by a triple $(\mathcal{V}, \mathbf{p}, K)$, consists of the following:

- $\mathcal{V} = \{1, \dots, n\}$ is the index set of n vertices (nodes) representing agents, sensors, etc., on the plane;
- $\mathbf{p} = \begin{bmatrix}\mathbf{p}_1^\top & \mathbf{p}_2^\top & \cdots & \mathbf{p}_n^\top\end{bmatrix}^\top \in \mathbb{R}^{2n}$ is the (position) *configuration* of the n vertices, with the assumption $\mathbf{p}_i = \mathbf{p}_j \Leftrightarrow i = j$, where $\mathbf{p}_i \in \mathbb{R}^2$ denotes the position of vertex i;
- $K = [k_{ij}]_{i,j\in\mathcal{I}} \in \mathbb{R}^{n\times n}$ is the *connectivity matrix*, where for each pair of vertices $i, j \in \mathcal{I}$, k_{ij} is the *connectivity coefficient* between them and satisfies $k_{ii} = 0$, $k_{ij} \geq 0$, and $k_{ij} = k_{ji}$. Denote by $\mathcal{K}$ the set of all such K.

Definition 2 (Anchored Formation Graph): A formation graph $(\mathcal{V}, \mathbf{p}, K)$ associated with a nonempty set $\mathcal{A} \subset \mathcal{V}$ is called an *anchored formation graph*, denoted by a quadruple $(\mathcal{V}, \mathbf{p}, K, \mathcal{A})$, where each vertex in $\mathcal{A}$ is called an *anchor* and each vertex in $\mathcal{F} \triangleq \mathcal{V} \setminus \mathcal{A}$ is called a *free vertex*.

We use the notations $\mathbf{p}_f \in \mathbb{R}^{2|\mathcal{F}|}$ and $\mathbf{p}_a \in \mathbb{R}^{2|\mathcal{A}|}$ to denote the components of $\mathbf{p}$ associated with free vertices and anchors, respectively.

In what follows, we define some quantities associated with a given (anchored) formation graph.

Definition 3: Let $\mathbf{r}^{(ij)} \in \mathbb{R}^{2n}$ be a column vector composed of n two-dimensional blocks,

$$\mathbf{r}^{(ij)} = \begin{bmatrix}\mathbf{0} & \cdots & \mathbf{0} & \underbrace{\mathbf{e}_{ij}^\top}_{i\text{-th block}} & \cdots & \underbrace{\mathbf{e}_{ji}^\top}_{j\text{-th block}} & \mathbf{0} & \cdots & \mathbf{0}\end{bmatrix}^\top,$$

where each $\mathbf{e}_{ij} \triangleq (\mathbf{p}_j - \mathbf{p}_i)/\|\mathbf{p}_j - \mathbf{p}_i\|$ is the unit direction vector pointing from $\mathbf{p}_i$ to $\mathbf{p}_j$. The *normalized rigidity matrix* R is defined to be the matrix whose rows are $\mathbf{r}^{(ij)\top}$ for $i, j \in \mathcal{V}$ such that $i < j$ and $k_{ij} > 0$.

Definition 4: The *(normalized) complete rigidity matrix* R^+ is defined to be the matrix whose rows are $\mathbf{r}^{(ij)\top}$ for *all* $i, j \in \mathcal{V}$ such that $i < j$.

Definition 5 ([11]): The *stiffness matrix* S is defined as

$$S \triangleq R^{+\top}\Lambda_K R^+, \tag{1}$$

where Λ_K is the diagonal matrix whose diagonal entries are the k_{ij} corresponding to the rows $\mathbf{r}^{(ij)\top}$ in R^+.

Proposition 1: The stiffness matrix S is positive semidefinite.

Proof: This can be readily seen from (1). ∎

Proposition 2: $\operatorname{rank}(R) = \operatorname{rank}(S)$.

Proof: According to Definition 5,

$$S = R^{+\top}\Lambda_K R^+ = \sum_{\substack{i,j\in\mathcal{V}\\ i<j}} k_{ij}\mathbf{r}^{(ij)}\mathbf{r}^{(ij)\top}$$

$$= \sum_{\substack{i,j\in\mathcal{V}\\ i<j, k_{ij}>0}} k_{ij}\mathbf{r}^{(ij)}\mathbf{r}^{(ij)\top} = R^\top\hat{\Lambda}_K R,$$

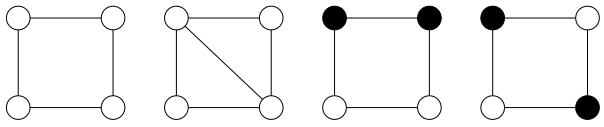

(a) Not rigid (b) Rigid (c) Not fixable (d) Fixable

Fig. 1. Examples illustrating rigidity and fixability

where $\hat{\Lambda}_K$ is the diagonal matrix whose diagonal entries are the *nonzero* k_{ij}. Therefore, $\hat{\Lambda}_K$ is positive definite, which implies the conclusion. ∎

Remark 1: The stiffness matrix S has the block structure $S = [S_{ij}]$, each $S_{ij} \in \mathbb{R}^{2\times 2}$ for $i, j \in \mathcal{V}$, where

$$\begin{cases} S_{ij} = -k_{ij}P_{ij}, & \text{if } i \neq j \\ S_{ii} = \sum_{j\in\mathcal{V}\setminus\{i\}} k_{ij}P_{ij}, \end{cases} \tag{2}$$

and $P_{ij} \triangleq \mathbf{e}_{ij}\mathbf{e}_{ij}^\top$ is the project matrix. Therefore, all the diagonal blocks are positive semidefinite, while each offdiagonal blocks are negative semidefinite, and each block row and block column adds up to zero. This structure resembles that of the well-known graph Laplacian [14].

The normalized rigidity matrix R can be partitioned as $R = \begin{bmatrix}R_f & R_a\end{bmatrix}$, where R_f contains all the block columns associated with the free vertices, and R_a contains all the block columns associated with the anchors. Likewise, the complete rigidity matrix R^+ can be split as $R^+ = \begin{bmatrix}R_f^+ & R_a^+\end{bmatrix}$. Moreover, according to (1), the stiffness matrix S can be partitioned similarly as follows,

$$S = \begin{bmatrix}R_f^{+\top}\\ R_a^{+\top}\end{bmatrix}\Lambda_K\begin{bmatrix}R_f^+ & R_a^+\end{bmatrix} = \begin{bmatrix}S_{ff} & S_{fa}\\ S_{af} & S_{aa}\end{bmatrix}. \tag{3}$$

Definition 6: A formation graph is called *infinitesimally rigid* (or simply *rigid* from now on) if $\operatorname{rank}(R) = 2n - 3$ [12], [13], or equivalently, $\operatorname{rank}(S) = 2n - 3$, due to Proposition 2.

Remark 2: An intuitive interpretation of the infinitesimal rigidity is that every infinitesimal perturbation which maintains the distances between connected vertices will only lead to a rigid-body motion in the three-dimensional subspace (translations and rotation), and hence will not deform the shape of the formation.

Definition 7 (Fixable Formation): An anchored formation graph $(\mathcal{V}, \mathbf{p}, K, \mathcal{A})$ is called *fixable* if S_{ff} is nonsingular.

Remark 3: A fixable formation can be viewed as an inflexible structure "pinned down" by the anchors, so that no infinitesimal perturbation on the free vertices may move them without violating the distance constraints.

Example 1: Some examples that illustrate the concepts of rigidity and fixability are given in Fig. 1. The black dots denote the anchors (which have fixed locations) and the white dots denote the free vertices. An edge between two vertices on the graph indicates that the connectivity coefficient between the two vertices is strictly positive. The unanchored formation in Fig. 1(a) is not rigid because, intuitively speaking, its shape can be deformed without changing the lengths of the edges, whereas in Fig. 1(b) the formation

has an inflexible structure and hence is rigid. Likewise, the anchored formation in Fig. 1(c) is not fixable, because the two free vertices on the bottom can be parallelly slided, without altering the lengths of the edges. The anchored formation Fig. 1(d) has all vertices locally fixed and hence is fixable.

III. Direction-Based Localization

In this section, the direction-based localization problem is formulated and analyzed, which is based on the following assumption.

Assumption 1 (Global Coordinate [9], [15]): There exists a global coordinate shared by all sensors/agents in the network in which the angles-of-arrival are measured.

The problem of direction-based localization with global orientation was previously formulated and studied in [8], [9] and recently in [15]. As follows, we provide an alternative formulation and analysis from the basis of the stiffness matrix and fixability property, on which the results in the next few sections depend.

Definition 8 (AOA Localization Problem): Assume that the absolute positions of the anchors $\mathbf{p}_a$ are known. Given the angle measurements $\theta_{ij} \in [0, 2\pi)$ for $(i,j) \in \mathsf{E}$, the AOA localization problem is to find solution $\mathbf{p}_f$ such that $\angle(\mathbf{p}_j - \mathbf{p}_i) = \theta_{ij}$ for all $i \in \mathcal{V}$, $j \in \mathcal{F}$ and $k_{ij} > 0$.

An AOA localization problem may have no feasible solution if the given angle measurements are inconsistent, as a trivial example, $|\theta_{ij} - \theta_{ji}| \neq \pi$. However, if we generate θ_{ij} from a given formation graph, then its own configuration must be admitted as one of possibly many solutions to the AOA localization problem.

Definition 9: An anchored formation graph is called *AOA localizable* if the AOA localization problem using θ_{ij} generated from the formation graph admits only one solution, which is its own configuration.

The key to the solution of the AOA localization problem is that $\mathbf{p}^\perp$ points in the direction of simultaneous rotation of the vertices around the origin. As a result, $\mathbf{p}^\perp \in \mathrm{null}(S)$, or

$$\begin{bmatrix} S_{ff} & S_{fa} \\ S_{af} & S_{aa} \end{bmatrix} \begin{bmatrix} \mathbf{p}_f^\perp \\ \mathbf{p}_a^\perp \end{bmatrix} = \mathbf{0}.$$

Particularly, the following equation holds true,

$$S_{ff}\mathbf{p}_f^\perp + S_{fa}\mathbf{p}_a^\perp = \mathbf{0}. \tag{4}$$

Assuming S_{ff} is nonsingular, the solution can be obtained by the following equation,

$$\mathbf{p}_f^\perp = -S_{ff}^{-1} S_{fa}\mathbf{p}_a^\perp. \tag{5}$$

We show that the above assumption is in fact necessary and sufficient for the uniqueness of the solution to the AOA localization problem.

Theorem 1 ([1]): An anchored formation graph is AOA localizable if and only if it is fixable.

Remark 4: The conclusion in Theorem 1 indicates that the solvability of a *direction-based* localization problem is determined by the fixability property in the *distance-based* localization framework (see Remark 3). This may shed light on the relation between the two localization paradigms.

IV. Discrete-Time Distributed Iterative Algorithm for AOA Localization

According to Theorem 1, Equation (5) provides a feasible and reliable method of solving the AOA Localization Problem. However, computing S_{ff}^{-1} is time-costly and technically difficult to carry out in a distributed fashion. To overcome this limitation, we decompose S_{ff} into $D_{ff} - F_{ff}$, where D_{ff} is composed of the 2×2 diagonal blocks in S_{ff} and F_{ff} the negated off-diagonal blocks. We first need to verify the invertability of matrix D_{ff}.

Proposition 3: If an anchored formation graph is fixable, then all 2-by-2 diagonal blocks of the matrix S_{ff} are invertible.

Proof: We prove by contraposition. Suppose a 2-by-2 diagonal block of S_{ff}, say S_{ii}, is singular. Recall from (2) that S_{ii} is the sum of the projection matrices. In the two-dimensional case, S_{ii} is singular if and only if all the projection matrices share the same null space. This implies that the null space shared by all the 2-by-2 blocks in the i-th block column and row is nontrivial. Therefore, S_{ff} must also be singular. ■

We assume that the anchored formation graph is fixable. By Proposition 3, D_{ff} is invertible. Therefore, (5) can be manipulated into the following iterative form,

$$\mathbf{p}_f^\perp = D_{ff}^{-1} F_{ff}\mathbf{p}_f^\perp - D_{ff}^{-1} S_{fa}\mathbf{p}_a^\perp. \tag{6}$$

We propose as follows a damped version of (6) which gives the same solution,

$$\mathbf{p}_f^\perp = (D_{ff} + \Lambda)^{-1} (F_{ff} + \Lambda)\, \mathbf{p}_f^\perp - (D_{ff} + \Lambda)^{-1} S_{fa}\mathbf{p}_a^\perp, \tag{7}$$

where Λ is assumed to be 2-by-2 block diagonal , i.e., $\Lambda = \mathrm{diag}(\Lambda_{ii})$ where $\Lambda_{ii} \in \mathbb{R}^{2\times 2}$. According to (2), we can write (7) in the decentralized form as below,

$$\mathbf{p}_i^\perp = \left(\Lambda_{ii} + \sum_{j \in \mathcal{V}\setminus\{i\}} k_{ij} P_{ij} \right)^{-1} \left(\Lambda_{ii}\mathbf{p}_i^\perp + \sum_{j \in \mathcal{V}\setminus\{i\}} k_{ij} P_{ij}\mathbf{p}_j^\perp \right) \quad \forall i \in \mathcal{F}.$$

The above expression can be viewed as the weighted average of the vectors $\mathbf{p}_i$ and $\mathbf{p}_j$ with matrix-valued weights Λ_{ii} and $k_{ij}P_{ij}$. Now we can design the following algorithm to solve (7) distributedly.

Remark 5: Algorithm 1 is essentially similar to a consensus process over the network. The subtle difference is that each node will converge to its respective localized position through the execution of the algorithm; whereas in the classical notion of consensus, all nodes converge to the same value over the network.

Let $\hat{\mathbf{p}}_f[k]$ in Algorithm 1 denote the estimated positions of the free vertices at step k. Note that the discrete-time dynamics of $\hat{\mathbf{p}}_f[k]$ can be expressed as below,

$$\hat{\mathbf{p}}_f^\perp[k+1] = (D_{ff} + \Lambda)^{-1} (F_{ff} + \Lambda)\, \hat{\mathbf{p}}_f^\perp[k] - (D_{ff} + \Lambda)^{-1} S_{fa}\mathbf{p}_a^\perp. \tag{8}$$

Algorithm 1 Distributed AOA Localization Algorithm for agent i at time step k

Input: $\Lambda_{ii} \in \mathbb{R}^{2\times 2},\ \hat{\mathbf{p}}_i^{\perp}[k],\ \hat{\mathbf{p}}_j^{\perp}[k],\ \theta_{ij} \in [0, 2\pi),\quad (j \in \mathcal{N}_i)$

Output: $\hat{\mathbf{p}}_i^{\perp}[k+1]$

$A \leftarrow \Lambda_{ii}$

$\mathbf{u} \leftarrow \Lambda_{ii}\hat{\mathbf{p}}_i[k]$

for all $j \in \mathcal{N}_i$ **do**

$\mathbf{e} \leftarrow [\cos\theta_{ij}, \sin\theta_{ij}]^\top$

$\mathbf{u} \leftarrow \mathbf{u} + \mathbf{e}\mathbf{e}^\top \hat{\mathbf{p}}_j^{\perp}[k]$

$A \leftarrow A + \mathbf{e}\mathbf{e}^\top$

end for

$\hat{\mathbf{p}}_i^{\perp}[k+1] \leftarrow A^{-1}\mathbf{u}$

We hereby define the convergence of the dynamics (8), thus equivalently, the convergence of the algorithm (that is, Algorithm 1).

Definition 10 (Convergence): Given an anchored formation graph $(\mathcal{V}, \mathbf{p}, K, \mathcal{A})$, if for any initial guess $\hat{\mathbf{p}}_f^{\perp}[0] \in \mathbb{R}^{2n}$, the dynamics (8) always converges to the true configuration $\mathbf{p}_f$, then we say that the algorithm is *convergent*.

It can be readily inferred from Theorem 1 that the fixability of the underlying formation graph is necessary for convergence. The following theorem gives a sufficient condition for convergence.

Theorem 2 (Sufficient Condition of Convergence): The algorithm is convergent if $(\mathcal{V}, \mathbf{p}, K, \mathcal{A})$ is fixable and Λ is symmetric positive definite.

Proof: Since $(\mathcal{V}, \mathbf{p}, K, \mathcal{A})$ is fixable, the convergence of the algorithm is implied by the stability of the discrete time-invariant affine system (8), which is given by

$$\rho\left(\left(D_{ff}+\Lambda\right)^{-1}\left(F_{ff}+\Lambda\right)\right) < 1,$$

where $\rho(\cdot)$ denotes the spectral radius. Since the matrix $\left(D_{ff}+\Lambda\right)^{-\frac{1}{2}}\left(F_{ff}+\Lambda\right)\left(D_{ff}+\Lambda\right)^{-\frac{1}{2}}$ is symmetric and similar to $\left(D_{ff}+\Lambda\right)^{-1}\left(F_{ff}+\Lambda\right)$, we can alternatively show that

$$I \succ \left(D_{ff}+\Lambda\right)^{-\frac{1}{2}}\left(F_{ff}+\Lambda\right)\left(D_{ff}+\Lambda\right)^{-\frac{1}{2}} \succ -I.$$

The first part of the inequality is easily seen given the positive definiteness of $\left(D_{ff}+\Lambda\right)^{-\frac{1}{2}}$ and $D_{ff}-F_{ff}$ (which is equal to S_{ff} and positive definite, by the assumption that the formation is fixable).

For the second part, it suffices to show that $D_{ff}+F_{ff}+2\Lambda \succ 0$. We observe that $D_{ff}+F_{ff}$ is the matrix whose off-diagonal blocks are negated compared to S_{ff}. Inspired by the following relation,

$$D_{ff}-F_{ff} = S_{ff} = R_f^{+\top}\Lambda_K R_f^{+},$$

we can see that $D_{ff}+F_{ff}$ can be similarly decomposed as follows,

$$D_{ff}+F_{ff} = \tilde{R}_f^{+\top}\Lambda_K \tilde{R}_f^{+}, \tag{9}$$

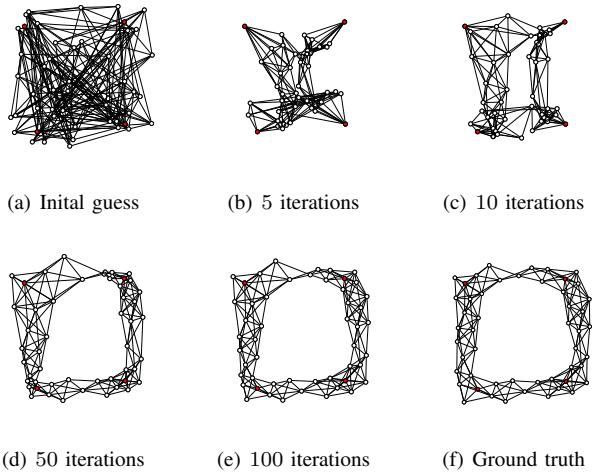

(a) Inital guess (b) 5 iterations (c) 10 iterations

(d) 50 iterations (e) 100 iterations (f) Ground truth

Fig. 2. Simulation result of the algorithm

where the matrix $\tilde{R}_f^{+}$ consists of rows in the following form

$$\tilde{\mathbf{r}}^{(ij)} = \big[\mathbf{0} \ \cdots \ \mathbf{0} \ \underbrace{\mathbf{e}_{ij}^\top}_{i\text{-th block}} \ \cdots \ \underbrace{\mathbf{e}_{ij}^\top}_{\substack{j\text{-th block}\\ \textit{(negated)}}} \ \mathbf{0} \ \cdots \ \mathbf{0}\big]^\top.$$

The decomposition in (9) certifies that $D_{ff}+F_{ff} \succeq 0$. Consequently, we have $D_{ff}+F_{ff}+2\Lambda \succ 0$. ■

A. Simulation

We test our distributed AOA localization algorithm on a multi-agent network consisting of 50 agents as shown in Fig. 3. Four agents at the corners of the formation (marked by red dots and labeled A, B, C and D) serve as anchors (i.e., their positions are *a priori* known). Fig. 2 shows the simulation result. As is theoretically proven, the localization result converges to the ground truth as the number of iterations increases.

V. Error Analysis

When the absolute positions of the anchors or the angle measurements are subject to error, Algorithm 1 still converges to the solution of (5), but the result may deviate from the ground truth. In this section, we study the effect of measurement error on the localization result through perturbational analysis. These results will be useful in assessing the steady-state performance of the algorithm, as well as formulating optimization problems in the future studies.

A. Inaccurate Anchor Locations

Consider the scenario where the absolute positions of the anchors differ from their true absolute positions by $\delta\mathbf{p}_a$. From (5) we can readily know that the localization error is

$$(\delta\mathbf{p}_f)^{\perp} = -S_{ff}^{-1}S_{fa}(\delta\mathbf{p}_a)^{\perp}.$$

From the above two relations, we propose two methods of evaluating the intensity of the error propagation from anchors' self-positioning to the AOA localization of free vertices. The first method is to regard $\delta\mathbf{p}_a$ as a static bias

and consider the largest possible error propagation due to $\delta\mathbf{p}_a$. We define the following *error propagation coefficient* for such worst case:

$$\varepsilon_a^{\mathrm{w}} \triangleq \max_{\delta\mathbf{p}_a\neq\mathbf{0}} \frac{\|\delta\mathbf{p}_f\|}{\|\delta\mathbf{p}_a\|} = \left\|S_{ff}^{-1}S_{fa}\right\|_2 \tag{10}$$

which is equal to the largest singular value of the matrix $S_{ff}^{-1}S_{fa}$.

A second method is to model the error $\delta\mathbf{p}_a$ as some random perturbation and consider the *root mean square error (RMSE)* of the localized positions, which can be computed as follows,

$$\begin{aligned}\sqrt{E\left[\|\delta\mathbf{p}_f\|^2\right]} &= \sqrt{\mathrm{tr}\left(S_{ff}^{-1}S_{fa}E\left[(\delta\mathbf{p}_a)^{\perp}(\delta\mathbf{p}_a)^{\perp\top}\right]S_{fa}^{\top}S_{ff}^{-1}\right)}\\ &= \sqrt{\mathrm{tr}\left(S_{ff}^{-1}S_{fa}Q\Sigma_{(\delta\mathbf{p}_a)}Q^{-1}S_{fa}^{\top}S_{ff}^{-1}\right)},\end{aligned} \tag{11}$$

where $\Sigma_{(\delta\mathbf{p}_a)}$ denotes the covariance matrix of $\delta\mathbf{p}_a$. Moreover, if each component of $\delta\mathbf{p}_a$ has an identical independent normal distribution $\mathcal{N}(0,\sigma_p^2)$, then the RMSE (11) can be further simplified as below,

$$\begin{aligned}\sqrt{E\left[\|\delta\mathbf{p}_f\|^2\right]} &= \sqrt{\sigma_p^2\cdot\mathrm{tr}\left(S_{ff}^{-1}S_{fa}S_{fa}^{\top}S_{ff}^{-1}\right)}\\ &= \sigma_p\cdot\left\|S_{ff}^{-1}S_{fa}\right\|_F,\end{aligned} \tag{12}$$

where $\|\cdot\|_F$ denotes the Frobenius norm of a matrix. Similar to the first case, we can also define the error propagation coefficient for the mean case as below,

$$\varepsilon_a^{\mathrm{m}} \triangleq \sqrt{E\left[\frac{\|\delta\mathbf{p}_f\|^2}{\|\delta\mathbf{p}_a\|^2}\right]} = \frac{1}{\sqrt{2|\mathcal{A}|}}\left\|S_{ff}^{-1}S_{fa}\right\|_F. \tag{13}$$

B. Inaccurate Angle Measurements

Let θ_{ij} denote the absolute angle of the incoming signal to vertex i from vertex j, for every $i\in\mathcal{F}$ and $(i,j)\in\mathcal{E}$. If there is no measurement error, then the relation $|\theta_{ij}-\theta_{ji}|=\pi$ holds. Consequently,

$$P_{ij} = \begin{bmatrix}\cos\theta_{ij}\\ \sin\theta_{ij}\end{bmatrix}\begin{bmatrix}\cos\theta_{ij}\\ \sin\theta_{ij}\end{bmatrix}^{\top} = P_{ji}.$$

Now we take the AOA measurement errors $\delta\theta_{ij}$ into account and apply perturbational analysis to (5). If both i and j are free vertices,

$$\begin{aligned}\frac{\partial(\delta\mathbf{p}_f)^{\perp}}{\partial\theta_{ij}} &= \frac{\partial(-S_{ff}^{-1})}{\partial\theta_{ij}}S_{fa}\mathbf{p}_a^{\perp}\\ &= S_{ff}^{-1}\frac{\partial S_{ff}}{\partial\theta_{ij}}\left(S_{ff}^{-1}S_{fa}\mathbf{p}_a^{\perp}\right) = -S_{ff}^{-1}\frac{\partial S_{ff}}{\partial\theta_{ij}}\mathbf{p}_f^{\perp},\end{aligned} \tag{14}$$

where the matrix derivative $\frac{\partial S_{ff}}{\partial\theta_{ij}}$ has only two nonzero blocks: $k_{ij}\frac{\partial P_{ij}}{\partial\theta_{ij}}$ at (i,i) and $-k_{ij}\frac{\partial P_{ij}}{\partial\theta_{ij}}$ at (i,j). Moreover,

$$\begin{aligned}\frac{\partial P_{ij}}{\partial\theta_{ij}} &= \begin{bmatrix}-\sin\theta_{ij}\\ \cos\theta_{ij}\end{bmatrix}\begin{bmatrix}\cos\theta_{ij}\\ \sin\theta_{ij}\end{bmatrix}^{\top} + \begin{bmatrix}\cos\theta_{ij}\\ \sin\theta_{ij}\end{bmatrix}\begin{bmatrix}-\sin\theta_{ij}\\ \cos\theta_{ij}\end{bmatrix}^{\top}\\ &= QP_{ij} + P_{ij}Q^{-1}.\end{aligned}$$

Plugging these into (14) and recalling that $P_{ij}(\mathbf{p}_i-\mathbf{p}_j)^{\perp}=\mathbf{0}$, we have

$$\begin{aligned}\frac{\partial(\delta\mathbf{p}_f)^{\perp}}{\partial\theta_{ij}} &= -S_{ff}^{-1}\begin{bmatrix}\\ k_{ij}(QP_{ij}+P_{ij}Q^{-1})(\mathbf{p}_i-\mathbf{p}_j)^{\perp}\\ \\ \end{bmatrix}\\ &= -k_{ij}S_{ff}^{-1}\begin{bmatrix}\\ \mathbf{p}_i-\mathbf{p}_j\\ \\ \end{bmatrix} \begin{array}{l}\leftarrow i\text{-th block row}\\ \text{(zero elsewhere)}\end{array}\\ &\triangleq -k_{ij}S_{ff}^{-1}\mathbf{w}_{ij}.\end{aligned} \tag{15}$$

The notation "|" here means that all components except the one specifically indicated are zero.

Next, we consider the case when j is an anchor, where both S_{ff} and S_{fa} now depend on θ_{ij}. With some calculation, it can be seen that

$$\frac{\partial(\delta\mathbf{p}_f)^{\perp}}{\partial\theta_{ij}} = -k_{ij}S_{ff}^{-1}\mathbf{w}_{ij}, \tag{16}$$

which turns out to be identical to the case when i,j are both free vertices.

We may stack all $\mathbf{w}_{ij}$ horizontally into the matrix W. Let $\delta\boldsymbol{\theta}$ be the vector whose components are $\delta\theta_{ij}$ and Λ_K be the diagonal matrices whose entries consist of k_{ij}, for all $(i,j)\in\mathcal{E}\cap(\mathcal{F}\times\mathcal{V})$. Then from (15) and (16) the total error can be written in the matrix form below,

$$\delta\mathbf{p}_f \approx Q^{-1}S_{ff}^{-1}W\Lambda_K\delta\boldsymbol{\theta}.$$

If the errors are modeled by the Gaussian random variables $\delta\theta_{ij}\sim\mathcal{N}\left(0,\sigma_{\delta\theta_{ij}}^2\right)$, the RMSE can be computed as below,

$$\begin{aligned}\sqrt{E\left[\|\delta\mathbf{p}_f\|^2\right]} &\approx \sqrt{\mathrm{tr}\left(S_{ff}^{-1}W\Lambda_K\Sigma_{\theta}\Lambda_K W^{\top}S_{ff}^{-1}\right)}\\ &= \left\|S_{ff}^{-1}W\Sigma_{\theta}^{\frac{1}{2}}\Lambda_K\right\|_F\end{aligned} \tag{17}$$

where $\Sigma_{\theta}\triangleq\mathrm{diag}\left(\sigma_{\delta\theta_{ij}}^2\right)$. We may define the error propagation coefficients for the worst case and the mean case (where we assume Σ_{θ} is isotropic) as follows,

$$\varepsilon_{\theta}^{\mathrm{w}} \triangleq \left\|S_{ff}^{-1}W\Lambda_K\right\|_2, \quad \varepsilon_{\theta}^{\mathrm{m}} \triangleq \frac{1}{\sqrt{2|\mathcal{E}|}}\left\|S_{ff}^{-1}W\Lambda_K\right\|_F.$$

C. Numerical Examples

To illustrate the results in the previous sections numerically, we computed the error propagation coefficients for the formation shown in Fig. 3 with different anchor sets. The four candidates for anchors are labeled A,B,C and D. The numerical results of the error propagation coefficients are listed in Table I.

From the numbers in Table I, several observations can be made. Firstly, the values of mean error propagation coefficients are always smaller than their worst-case counterparts, which verifies their definitions. Secondly, one may notice that in general the more anchors the network possesses, the smaller $\varepsilon_{\theta}^{\mathrm{w}}$ and $\varepsilon_{\theta}^{\mathrm{m}}$ becomes. This complies with our intuitive that more anchors help suppress the uncertainty caused by measurement errors. Particularly, in the case of A,B being the anchors, the localization errors caused by inaccurate AOA

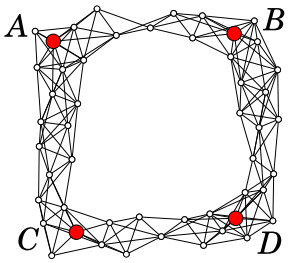

Fig. 3. Sample anchored formation graph (ground truth)

TABLE I
ERROR PROPAGATION COEFFICIENTS FOR FIG. 3

Anchor Set	$\varepsilon_a^{\mathrm{w}}$	$\varepsilon_a^{\mathrm{m}}$	$\varepsilon_\theta^{\mathrm{w}}$	$\varepsilon_\theta^{\mathrm{m}}$
A, B, C, D	5.8885	3.8852	6.5043	2.8913
A, B, C	5.4307	3.9999	15.1156	6.9432
A, B	9.2271	5.8950	184.1435	92.5459
A, D	5.0222	4.5624	24.1448	13.2067

measurements could potentially be huge. This can be seen intuitively from Fig. 3, as the wing on the bottom is hardly "pinned down" by any anchors, and hence can be easily deformed.

The numerical results regarding the error propagation coefficients for the anchor position errors are relatively harder to interpret. It can be seen from the first, second and fourth cases in Table I that more anchors may cause larger error on the localization result in general. Nevertheless, a small but poorly chosen anchor set, such as the third case, could still potentially lead to large error propagation coefficients. These results motivate us to further investigate the factors which affect the error propagation coefficients, and the formulation of optimization problems with respect to these coefficients in the future.

VI. CONCLUSION

In this paper, we propose a discrete-time distributed algorithm for network localization based on angle-of-arrival (AOA) measurements. This algorithm can be viewed as a special case of the averaging consensus algorithm in the two-dimensional space. The effectiveness of our localization algorithm is demonstrated through numerical simulation. We also analyze the localization error under inaccurate anchor positions and angles measurements and provide approximate formula for the error term. Numerical examples are provided to illustrate the relation between the anchored formation graphs and their the error progagation coefficients.

Compared to other sophisticated AOA localization methods [16], our algorithm may typically require more iterations to converge to a relatively precise configuration. An explanation for this is that, our current scheme does not weigh the information according to its confidence when it is taken into weighted-average-like computation. Therefore, we can imagine that the algorithm may take a lot of iterations to counter the effect of the initial guess. To improve the algorithm in the future, we may dynamically adjust the link connectivity coefficients k_{ij} based on the confidence level of the node. The effect of the damping matrix Λ is also a quantity that we will look into in our future work. Based on the theorical framework of our algorithm proposed in this paper, we expect that more performance improvements can be made through optimization with respect to quantities such as the above-mentioned K and Λ.

REFERENCES

[1] G. Zhu and J. Hu, "Distributed network localization using angle-of-arrival information Part I: Continuous-time protocol," in *Proceedings of the 2013 American Control Conference*, June 2013.

[2] R. Collins, A. Lipton, T. Kanade, H. Fujiyoshi, D. Duggins, Y. Tsin, D. Tolliver, N. Enomoto, O. Hasegawa, P. Burt *et al.*, *A system for video surveillance and monitoring*. Carnegie Mellon University, the Robotics Institute, 2000.

[3] L. Bodrozic, D. Stipanicev, and M. Stula, "Agent based data collecting in a forest fire monitoring system," in *International Conference on Software in Telecommunications and Computer Networks (SoftCOM)*, October 2006, pp. 326–330.

[4] N. Patwari, J. Ash, S. Kyperountas, I. Hero, A.O., R. Moses, and N. Correal, "Locating the nodes: cooperative localization in wireless sensor networks," *IEEE Signal Processing Magazine*, vol. 22, no. 4, pp. 54–69, July 2005.

[5] N. B. Priyantha, A. Chakraborty, and H. Balakrishnan, "The Cricket location-support system," in *Proceedings of the 6th annual international conference on Mobile computing and networking*, ser. MobiCom. New York, NY, USA: ACM, 2000, pp. 32–43.

[6] C. Savarese, J. Rabaey, and J. Beutel, "Location in distributed ad-hoc wireless sensor networks," in *Proceedings of IEEE International Conference on Acoustics, Speech, and Signal Processing (ICASSP)*, vol. 4, 2001, pp. 2037–2040.

[7] T. Eren, O. Goldenberg, W. Whiteley, Y. Yang, A. Morse, B. Anderson, and P. Belhumeur, "Rigidity, computation, and randomization in network localization," in *INFOCOM*, vol. 4, March 2004, pp. 2673–2684.

[8] J. N. Ash and L. C. Potter, "Robust system multiangulation using subspace methods," in *Proceedings of the 6th International Conference on Information Processing in Sensor Networks*, ser. IPSN '07. New York, NY, USA: ACM, 2007, pp. 61–68.

[9] T. Eren, W. Whiteley, and P. Belhumeur, "Using angle of arrival (bearing) information in network localization," in *Proceedings of the 45th IEEE Conference on Decision and Control*, Dec. 2006, pp. 4676–4681.

[10] J. Chen, K. Yao, and R. Hudson, "Source localization and beamforming," *IEEE Signal Processing Magazine*, vol. 19, no. 2, pp. 30–39, March 2002.

[11] G. Zhu and J. Hu, "Stiffness matrix and quantitative measure of formation rigidity," in *Proceedings of the 48th IEEE Conference on Decision and Control, held jointly with 28th Chinese Control Conference*, December 2009, pp. 3057–3062.

[12] W. Whiteley, "Some matroids from discrete applied geometry," in *AMS-IMS-SIAM Joint Summer Research Conference on Matroid Theory*, vol. 197. University of Washington, Seattle: American Mathematical Society, July 1995, pp. 171–311.

[13] B. Jackson and T. Jordán, "Connected rigidity matroids and unique realizations of graphs," *Journal of Combinatorial Theory, Series B*, vol. 94, no. 1, pp. 1–29, 2005.

[14] M. Mesbahi and M. Egerstedt, *Graph Theoretic Methods in Multiagent Networks*. Princeton University Press, 2010.

[15] A. N. Bishop, I. Shames, and B. D. Anderson, "Stabilization of rigid formations with direction-only constraints," in *Proceedings of the 50th IEEE Conference on Decision and Control and European Control Conference*, December 2011, pp. 746–752.

[16] P. Rong and M. Sichitiu, "Angle of arrival localization for wireless sensor networks," in *3rd Annual IEEE Communications Society on Sensor and Ad Hoc Communications and Networks*, vol. 1, September 2006, pp. 374–382.